Inversion for geometric and geoacoustic parameters in shallow water: Experimental results

Donald F. Gingras and Peter Gerstoft
SACLANT Undersea Research Centre, 19138 La Spezia, Italy

(Received 4 November 1994; accepted for publication 15 February 1995)

Experimental results on the estimation of both geometric and geoacoustic parameters in shallow water are presented. Genetic algorithms are used for estimation of the forward model parameters; the estimated parameters are then used by a standard Bartlett processor for source localization. A stationary source at a range of 5.6 km and a moving source at ranges from 5.8–7.7 km were successfully localized in range and depth using a single frequency Bartlett processor. The results indicate that global estimation of the forward model parameters significantly improves source localization performance.

PACS numbers: 43.30.Wi, 43.60.Pt

INTRODUCTION

The inversion of acoustic field data using the "matched-field" processing method is a widely accepted procedure for estimating both geometric and geoacoustic parameters. The so-called "matched-field" method simply implies that acoustic field observations are "matched" in some sense to multiple iterations of a forward model as a function of search parameters. This form of processing has been applied to a variety of estimation problems including source localization; see, for example,[1–7] tomography,[8] and inversion for ocean and ocean bottom properties.[9–13] In many cases the "matching" is accomplished via a correlation process often referred to as the linear or Bartlett processor.

In general, there is no direct solution for the estimation of ocean and bottom parameters from acoustic field observations. Often this inverse problem is posed as a nonlinear optimization problem. The problem is formulated by assuming a discrete forward model parameter vector $\mathbf{m}=\{m_i\}$ of unknown parameters with a bounded range of possible values for each parameter. An objective function which provides a measure of the similarity between the observed field and the field predicted via forward modeling is optimized with respect to the model vector. In most situations the model parameter search space is extremely large; thus solution via exhaustive search is not a viable option. Furthermore, the objective function may contain many local minima precluding the use of gradient decent methods. Efficient global optimization methods such as simulated annealing (SA) and genetic algorithms (GA) must be employed.[9–13]

Collins and Kuperman were the first to include the "environmental" parameters into the search space for source localization.[9] Simulation results were presented which demonstrated the utility of using SA to search the expanded search space. In Ref. 10 SA was applied to the estimation of ocean-bottom properties; successful results were obtained using experimental data. References 11 and 12 provided results based on simulations for the estimation of ocean-bottom properties using SA. The first application of GA methods to the estimation of geoacoustic parameters was by Gerstoft,[13] where successful results were obtained using synthetic data.

There have been a number of papers reporting on experimental results for the estimation of source location parameters in shallow water using matched-field processing. In 1989 Hinich and Sullivan[2] reported a localization based on a mode filtered maximum likelihood method. Only a single localization was reported and for this case the depth estimate was not correct. They reported that the lack of results was perhaps due to array motion. Ozard[3] reported on a localization involving a short horizontal array. There were no reliable range estimates reported but the depth estimation results were encouraging. Hampson and Heitmeyer[4] reported on source localizations in shallow water. In this case three successful localizations were reported, all at different frequencies. In all three cases the sidelobe level was very close to that of the source peak. In 1990 Feuillade *et al.*,[5] reported a single shallow water localization in very shallow water (33 m) using the Capon maximum likelihood processor. In 1993 Jesus[6] reported on successful source localizations for transient signals. Reasonably accurate estimates for both range and depth were reported. The results of Ref. 6 were the only shallow water results that reported consistent range and depth estimates over time. In all of the above, the geoacoustic parameters were assumed to be known and were not estimated as part of the localization process.

In October 1993 the SACLANT Centre conducted a sea trial in the Mediterranean Sea using a vertical array in shallow water. The trial was conducted in an area where the geoacoustic properties were reasonably well known from previous SACLANT Centre experiments.[14–16] An objective of the October 1993 experiment was to verify the performance of field inversion methods in shallow water under somewhat optimal conditions, i.e., an array that spanned most of the water column, knowledge of hydrophone positions via array positioning, a stationary and moving source, and *a priori* knowledge of the geoacoustic parameters.

Based on the successful results of Ref. 13 this paper focuses on the estimation of source location parameters using GA as a preprocessor for estimation of the other forward model parameters. Since the geometric and geoacoustic pa-

rameters cannot be decoupled, global estimation methods were first used to jointly estimate both types of parameters. Then the forward model parameters were used in a standard matched-field processor for source localization. The use of the GA estimates significantly improved source localization results as compared to those obtained without the estimated model parameters. This paper provides successful results on the estimation of both geometric and geoacoustic parameters using GA with experimental data in shallow water.

For any parameter estimation problem the issue of error analysis must be addressed. There are a variety of methods for evaluating error estimates which have been established for local inverse theory; many of these methods are not well suited for global optimization.[17] In Refs. 13 and 17 the use of *a posteriori* distributions constructed from the samples of the search space was shown to be effective for global approaches. In this analysis *a posteriori* distributions were used to provide error estimates and an indication of the relative importance of the parameters.

In Sec. I a brief summary of the trial site and equipment deployed is provided. In Sec. II a brief overview of GA is presented along with the results obtained for the geometric and geoacoustic parameter inversion. In Secs. III and IV the source localization results, based on the estimated forward model parameters, are presented for a stationary and moving source. Finally, in Sec. V a discussion of the results is presented.

I. EXPERIMENTAL SETUP

The experimental data were collected over a 2-day period on 26 and 27 October 1993 in a shallow water area north of the island of Elba, off the Italian west coast, where environmental conditions were known from earlier SACLANT Centre experiments.[14–16] This area is characterized by a flat bottom covered with clay and sand-clay sediments. The trial was conducted in a flat area between the 120- and 140-m depth contours along a track running parallel to the depth contours. The propagation conditions were typical downward refracting summer conditions. The weather over the 2-day period was favorable, a sea state of 2 to 3, the wind on the 26th was variable between 6 and 10 m/s and on the 27th it averaged about 3 m/s.

On the morning of the 26th the vertical array, array positioning transponders, and a stationary source buoy were deployed. On the afternoon of the 27th a support ship, the ITN PALMARIA, provided a moving source along the track indicated by points A and B in Fig. 1. Figure 1 also indicates the relative locations for the vertical array and the source buoy along with the local bathymetry. Acoustic field data from the two sources, array positioning data, sound-speed profile and current versus depth profile data were acquired over the 2-day period.

A. Vertical array and array positioning

The vertical array was deployed at 43° 02.86′ N 10° 10.01′ E. Due to the accuracy of the GPS system on board the R/V ALLIANCE the position of the vertical array is only known within ±100 m. The bathymetry was measured to be approximately 127 m at the array site. The vertical array was

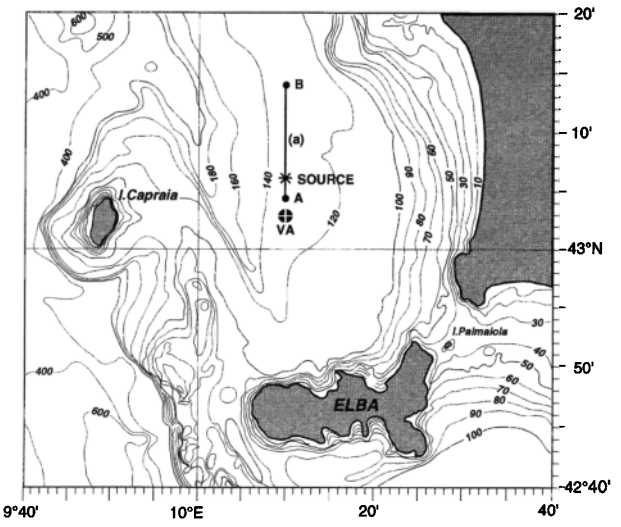

FIG. 1. Bathymetry, equipment locations and ship track.

deployed in a bottom moored configuration with ballast and a subsurface low-drag float; see Fig. 2. The multichannel array hydrophone data were digitized in the array, transmitted via a cable to a surface buoy and then transmitted via a radio link to the real-time processing and archival storage system on board the R/V ALLIANCE. The vertical array had a total aperture of 94 m, within the 94 m aperture a total of 48 hydrophones with 2-m spacing were used. Based on the physical configuration shown in Fig. 2 and the measured bathymetry of 127 m at the array site the bottom hydrophone was at a depth of 112.7 m. The hydrophone closest to the surface was correspondingly at a depth of 18.7 m. These are nominal depths based on the above assumptions; the actual depths were different due to array tilt, imprecise measurement of the bathymetry and ballast penetration into the sediment.

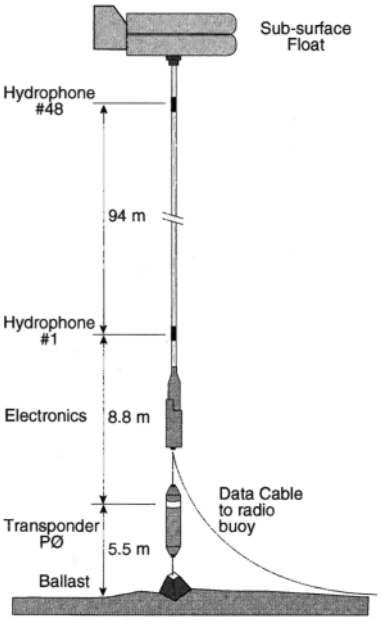

FIG. 2. The SACLANT Centre vertical array as deployed in a bottom moored configuration.

In order to determine the variation of the array hydrophone positions in the water column due to tilt an acoustic array positioning system was deployed with the vertical array. The array positioning hardware consisted of four acoustic transponders and a shipboard interrogation unit. Three transponders were deployed around the vertical array at a range of approximately 250 m in an approximate equilateral triangle configuration. Each transponder was bottom moored with ballast and subsurface floats to keep the transponders a few meters (5.5 m) from the bottom. A fourth transponder was attached to the bottom of the vertical array. The time of arrival information obtained by analyzing the vertical array data (subset of eight hydrophones) from the four transponders was sufficient to localize the transponders with respect to each other and the array hydrophone positions in a local coordinate system. A detailed description of the array positioning system and methods is available in Ref. 18.

Estimates of array shape for the 26th at four time samples were calculated by the array positioning system. For the first three time samples the maximum deflection from vertical was on the order of 0.75 m and it occurred at the top of the array. For the fourth time sample the maximum was somewhat greater, i.e., 0.98 m, again at the top of the array. Estimates for the 27th at four time samples were also computed. On the 27th the average maximum deflection from vertical was on the order of 0.4 m; the location of the maximum deflection was in the mid portion of the array. This degree of deflection from vertical was sufficiently small with respect to a wavelength at the frequencies of interest that array shape correction was not required.

B. Source and signal characteristics

The stationary source was deployed approximately 5.6 km due north of the vertical array. The source was suspended from a buoy which was tethered to a ballast on the bottom. At the source location the bathymetry was measured to be 130 m.

One of the signals transmitted by the stationary source was a continuous transmission of pseudorandom noise (PRN) produced using a maximal length sequence (MLS) based on a six bit shift register and bit length of 52.9-ms modulated onto a carrier with center frequency of 170 Hz. The repetition length for this sequence was 3.15 s, the −3-dB bandwidth was approximately 12 Hz, and the source level was approximately 163 dB *re*: 1 μPa/$\sqrt{\text{Hz}}$. For further information on MLS see, for example, Ref. 19.

On the afternoon of the 27th a source ship towed a source from point A to point B (Fig. 1) at a speed of approximately 3.5 kn. One of the signals transmitted by the source was a PRN sequence similar to that discussed above. The source level was approximately 176 dB *re*: 1 μPa/$\sqrt{\text{Hz}}$. This signal was transmitted for 30 s out of every minute.

Over the course of the 2 days the sources transmitted a variety of signal types in two frequency bands, a band from 160 to 180 Hz and from 320 to 350 Hz. For the analysis reported herein a signal in the 160- to 180-Hz band was selected. For the stationary source a 39 min sequence of the PRN signal was processed (15:44 to 16:23 on 26 October).

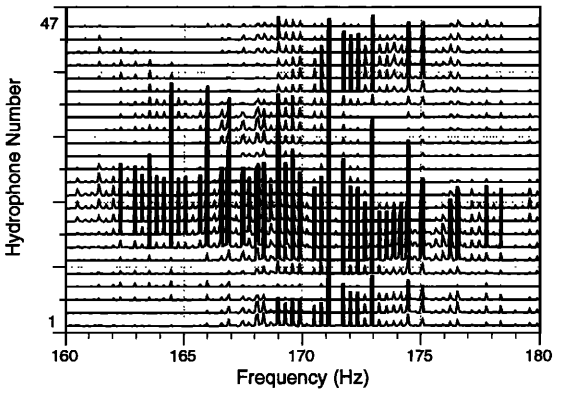

FIG. 3. Spectrum for the stationary source PRN signal as received on the vertical array at $T=0$ min, odd numbered hydrophones only.

For the moving source a 17-min sequence of the PRN signal was processed (14:41 to 14:58 on 27 October).

Figure 3 illustrates an example of the PRN signal in the frequency domain as a function of hydrophone number (odd-numbered hydrophones only) for a 16-s sample. Note the discrete "pickets" in frequency which are characteristic of the spectrum of PRN signals. Examining Fig. 3 it is seen that the signal-to-noise ratio is highly variable across the array and as a function of frequency. At the center of the band, slightly below 170 Hz, there is a "picket" with energy across most of the array, this portion of the signal centered at 169.9 Hz was used throughout the analysis.

II. GA PARAMETER ESTIMATION

Genetic algorithms are based on an analogy with biological evolution. The basic principle of GA is simple: From all possible model vectors, an initial population of q members is selected. The fitness (or objective function) of each member is computed. Then, through a set of evolutionary steps, the initial population evolves in order to become more fit. An evolutionary step consists of selecting a parental distribution from the initial population based on the individual's fitness. The parents are then combined in pairs, and operators are applied to them to form a set of children. The operators are the crossover and mutation operators. Finally, the children replace part of the initial distribution to get a more fit population. For a detailed description of GA and their application to geoacoustic parameter estimation, see Ref. 13.

A. Baseline environmental model

The environmental model consisted of an ocean layer overlying a sediment layer and a bottom layer as shown on Fig. 4. All layers were assumed to be range independent. For the purposes of the inversion the forward model parameters were subdivided into four parameter subsets: Geometric, sediment, bottom, and water sound speed. The geometric parameters included source range, source depth, the depth of the receiver array and bathymetry. The baseline sediment and bottom properties used for the North Elba site were based on the work of Jensen,[16] see Fig. 4. Note that the sediment and bottom parameters are average parameters determined by

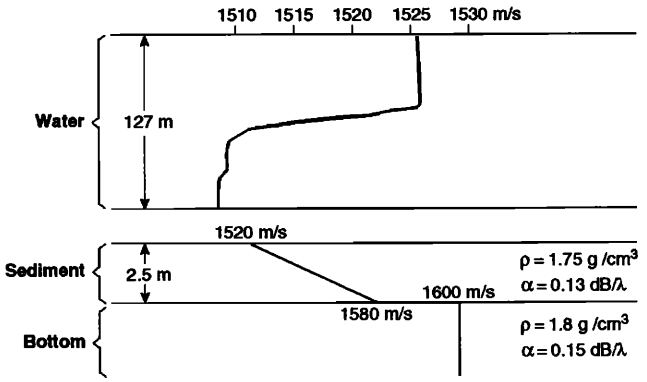

FIG. 4. Measured sound-speed profile and bathymetry with historical geoacoustic parameters for the North Elba experiment site, geoacoustic parameters are from Ref. 16.

matching predicted transmission loss with measured transmission loss in the North Elba basin over a wide range of frequencies; see Ref. 16. For this area Jensen[16] obtained good agreement between predicted and experimental propagation loss without including shear properties; thus shear properties were not included in the model. The water sound-speed profile was from a CTD taken near the vertical array on the morning of 26 October. As seen in Fig. 4 the water sound-speed profile was a summer profile, almost isovelocity down to 60 m and then a strong thermocline extending to about 80 m. Optimization was not carried out over the water sound-speed profile. The baseline value for receiver depth was based on the bathymetry measured at the array and the physical characteristics of the array and mooring (see Fig. 2).

The baseline forward model of Fig. 4 was used with the SACLANTCEN normal mode propagation model, SNAP,[20] to predict the normal mode structure for a source at 170 Hz at a depth of 80 m. The magnitude of the vector inner product of the depth sampled mode eigenfunctions and the SNAP predicted pressure field at a range of 5.6 km was evaluated. At this range mode 2 was the dominant mode with modes 1 and 5 also contributing. Modes 6, 7, and 8 provided a contribution but at a much reduced level. Thus the inversion was based primarily on the contribution of three modes.

B. Objective function

The inverse problem was solved as an optimization problem; that is, find the model vector $\mathbf{m}=\{m_i\}\ i=1,2,\ldots,p$ that minimized the objective function. The objective function was a function of the vector of observations $\mathbf{q}$ and a vector of forward model predictions $\mathbf{w}(\mathbf{m})$. The following normalized Bartlett processor was used:

$$P(\mathbf{m};\omega_j)=\frac{\mathbf{w}^*(\mathbf{m})\hat{\mathbf{R}}(\omega_j)\mathbf{w}(\mathbf{m})}{\|\mathbf{w}(\mathbf{m})\|^2}, \tag{1}$$

where $\hat{\mathbf{R}}(\omega_j)$ is the data cross-spectral matrix formed from the observation vectors at a single frequency ω_j.

The time series data for the 48 hydrophones were used to estimate the cross-spectral matrices. The data for each hydrophone were transformed into the frequency domain using a Fourier transform. Since the data were acquired at a sample rate of 1 kHz and the transform length was 4096 samples the "bin" width was 0.24 Hz. The cross-spectral matrix was formed near the center frequency of the signal band, 169.9 Hz. Each matrix was computed as an inner product of the observation vectors ($\mathbf{q}^*,\mathbf{q}$) normalized by the norm of the observation vector squared. An average over two time epochs was computed; thus each matrix represented a total time sample of approximately 8 s. An estimate of the cross-spectral matrix was calculated at 1 min intervals over the stationary data time period yielding 40 cross-spectral matrix estimates.

TABLE I. GA forward model parameters with search bounds.

Model parameter	Lower bound	Upper bound
Geometric		
source range (m)	5200	5600
source depth (m)	70	85
receiver depth (m)	110	114
bathymetry (m)	125	130
Sediment		
comp. speed, upper (m/s)	1450	1550
comp. speed, lower (m/s)	1500	1600
density (g/cm^3)	1.2	2.2
attenuation (dB/λ)	0.0	0.4
thickness (m)	0.0	6.0
Bottom		
comp. speed (m/s)	1550	1650
density (g/cm^3)	1.2	2.2
attenuation (dB/λ)	0.0	0.4

C. Model parameter estimation

There are a few GA parameters that must be defined for each GA application. Based on previous experience the following values were used in the analysis of the North Elba data; see Ref. 13. The population size was set to 64, the reproduction size was 0.5, the crossover probability was 0.8, the mutation probability was 0.05, and the number of iterations (or forward model computations) was 2000. The forward model used was the range-independent SNAP model.[20] One "inversion" consisted of 2000 forward model computations for each of ten independent parallel populations. Thus a total of 20 000 forward model computations were used for each inversion. Each inversion (20 000 forward models) required 9 min of CPU time on a DEC 3000/800 Workstation, about 90% of the CPU time was used for forward model computations.

The optimization was carried out using 12 parameters (see Table I), which are grouped into three subsets: geometric, sediment, and bottom. Table I also provides the search bounds used for each parameter. For each parameter the search space was quantized into 128 increments. There was no optimization of the water sound-speed profile; a single sound-speed profile based on a CTD measurement at the array site was used. The interpretation of the parameters of Table I is quite straightforward except for "receiver depth." The receiver depth is the depth of the deepest hydrophone; the GA used this parameter to optimize the vertical position of the entire vertical array in the water column. Twelve parameters with a quantization of 128 steps results in a search

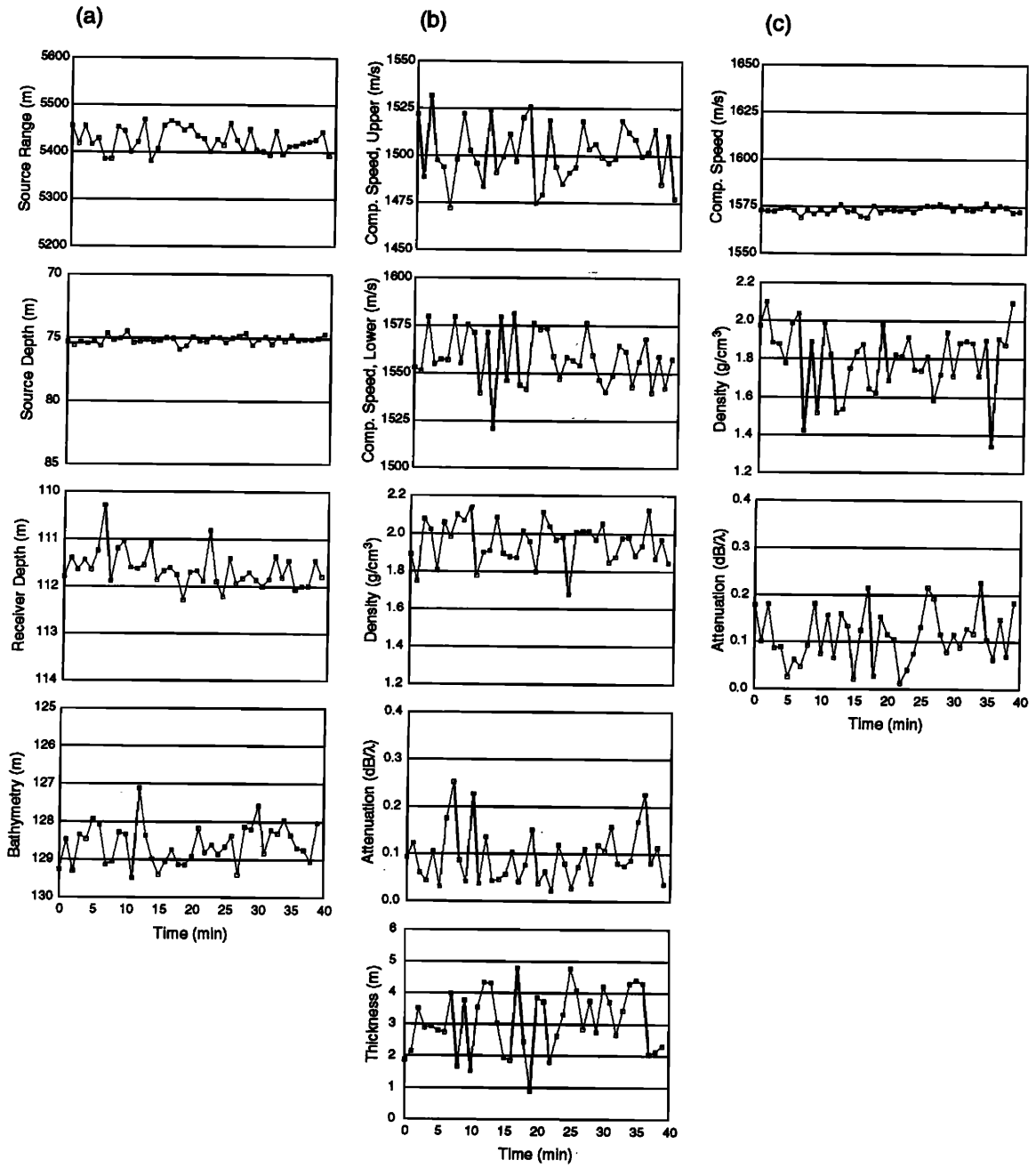

FIG. 5. GA *a posteriori* mean as a function of time: (a) geometric, (b) sediment, and (c) bottom parameters.

space containing $128^{12} \approx 10^{25}$ samples, as discussed above; only 20 000 models were computed. Thus only a small fraction of the search space was sampled.

Inversion for the 12 geometric and geoacoustic parameters was carried out for each of the 40 cross-spectral matrices. For each of the 40 samples the GA produced 320 model estimates (population size times number of parallel populations times reproduction size). Figure 5 illustrates the GA mean [see Eq. (12) of Ref. 13], computed over the 320 most fit estimates, for each of the 12 parameters as a function of time. The range of values plotted is the same as the parameter search bounds. Since the source and receiver were both fixed the variability of the mean estimate as a function of time was used as a measure of consistency. It is seen that the geometric parameters—Fig. 5(a)—were fairly consistent over time, especially source depth. Examining Fig. 5(b) it is seen that the sediment parameter estimates were not consistent; even the upper and lower compressional speeds were highly variable. From Fig. 5(c) it is seen that the compressional speed for the bottom was consistent but the bottom density and attenuation estimates were not.

In order to obtain a single estimate for each of the 12 parameters the 320 parameter estimates for each of the 40 time samples were concatenated into one collection of samples. *A posteriori* probability distributions for each of the 12 parameters were estimated using the 320×40 samples; see Fig. 6. These distributions provide additional insight into the performance of the parameter inversion process. Clearly, the results provided by Figs. 5 and 6 are closely related. They use the same data, but Fig. 5 emphasizes the variability

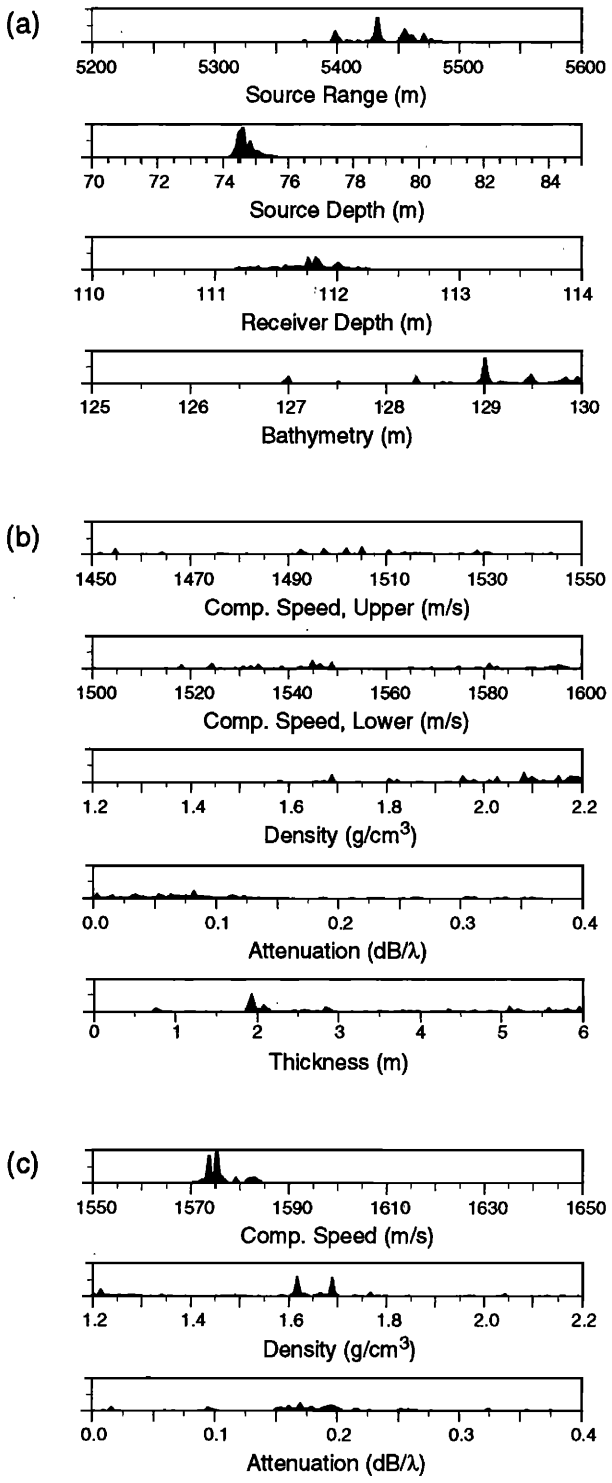

FIG. 6. *A posteriori* probability distributions for each of the 12 model parameters based on the 40 observations: (a) geometric, (b) sediment, and (c) bottom parameters.

of the estimates as a function of time whereas Fig. 6 emphasizes the variability over the search interval. It is seen that the source range and depth, bathymetry, receiver depth, and compressional speed in the bottom are quite well determined. That is, the distributions are compact over the search interval, and there is an unambiguous peak indicating that the inversion was fairly successful at finding a good fit for these parameters. The sediment layer was not very deep, less than one-third of a wavelength; thus the propagation was not sensitive to this layer and the sediment parameters were not well determined. As shown in Ref. 21 those parameters which were not well determined are also those parameters for which accurate knowledge is not required for source localization.

TABLE II. Baseline model parameters and GA parameter estimates based on 40 observations and a reliability measure.

Model parameter	Baseline	GA mean	Reliability
Geometric			
source range (m)	5600	5437	0.07
source depth (m)	80.0	74.6	0.02
receiver depth (m)	112.7	111.7	0.06
bathymetry (m)	127.0	128.9	0.17
Sediment			
comp. speed, upper (m/s)	1520	1505	0.24
comp. speed, lower (m/s)	1580	1556	0.27
density (g/cm^3)	1.7	2.0	0.19
attenuation (dB/λ)	0.13	0.11	0.20
thickness (m)	2.5	3.3	0.26
Bottom			
comp. speed (m/s)	1600	1576	0.04
density (g/cm^3)	1.8	1.6	0.23
attenuation (dB/λ)	0.15	0.18	0.20

Based on the *a posteriori* probability distributions, three estimates for the model parameters are available: those associated with the largest fitness, those based on the peak of the distribution and those based on the mean of the distribution. Analysis of the estimated parameters has shown that the mean is the most robust; thus it was used as the parameter estimate (see Table II). Table II also contains the baseline parameters and a reliability measure which indicates how well each parameter has been determined. The reliability measure is the standard deviation of the distribution expressed as a fraction of the search interval for each parameter. This measure describes how well the estimates are clustered within the search interval. The reliability measure supports the conclusions discussed above, namely that the geometric parameter estimates are consistent, the sediment estimates are not consistent, and the bottom compressional speed estimate is very consistent.

Comparing the baseline model parameters with the GA estimated parameters, it is apparent that there are some differences between the baseline and estimated values. For the geometric parameters the estimated location of the deepest hydrophone differs by 1 m from the measured value. The estimated bathymetry is an "average" bathymetry as seen by the acoustic field. The estimated value falls between the measured values at the source and receiver. The geoacoustic values are also somewhat different. This is not surprising since the baseline geoacoustic values are average values obtained by averaging over a wide range of frequencies and ranges, whereas the estimated values were obtained at a single frequency and range.

The selection of the search bounds used for parameter estimation (see Table I) is dependent on the estimation objective and *a priori* knowledge. In this section the objective

was the estimation of the nonsource related parameters; thus fairly tight bounds were used for the source range and depth. If the objective had been the estimation of source location parameters, then the bounds on those parameters would have been much broader; see, for example, Ref. 22.

III. STATIONARY SOURCE LOCALIZATION

In this section we examine the performance of matched-field processing for estimation of source location parameters using the vertical array data obtained during the October 1993 sea trial. The standard Bartlett processor was used to generate estimates of source range and depth. The Bartlett processor was computed using both the baseline and GA estimated values for the forward model parameters. A search over source range and depth was performed to generate ambiguity surfaces. The location of the maximum of the ambiguity surface was used as the source location parameter estimate. The Bartlett processor was normalized such that a perfect match between the predicted field and the observed field yielded a maximum value of 0 dB; see Eq. (1). The analysis was carried out for a single frequency centered at 169.9 Hz. The water sound-speed profile was that shown in Fig. 4 measured at the vertical array site on the morning of the 26th.

The data were the 39-min sample (48 hydrophones) of the PRN signal collected using the stationary source on 26 October (same data as used by the GA to estimate model parameters). The hydrophone positions were not corrected for tilt; the acoustic positioning estimates of array shape indicated that the tilt was always less than 1 deg. Based on the known uncertainties about the GPS position for the vertical array and the source buoy, the source range with respect to the vertical array was predicted to be 5600 ± 200 m. The accuracy of the knowledge about the source depth would lead to a prediction of 80 ± 2 m.

A. Performance versus model

Comparing the model parameters of Table II, i.e., the baseline and the GA estimated parameters, it was of interest to understand which model parameters were important with respect to obtaining a good field match between the predictions and the field observations. As a starting point the 40 samples of the PRN signal were processed using a number of model vectors. The search space was limited to a small region containing the source, 5 to 6 km in range and 10 to 100 m in depth. Figure 7 is the power of the Bartlett processor at the maximum of the ambiguity surface as a function of time. Line (1) is the result obtained evaluating the Bartlett power versus time using the baseline model. Line (2) illustrates the power when the GA estimated bathymetry and receiver depth are used in place of the baseline values. Comparing line (1) with line (2) it is seen that using the GA estimated values produced a better match. By changing the bathymetry from 127 m to the estimated value of 128.9 m and the receiver depth from 112.7 to 111.7 m the mean Bartlett power increased from -2.7 to -0.9 dB. Most of the improvement was due to the estimate of bathymetry. Using only the bathymetry estimate the mean Bartlett power was -1.2 dB. Line (3), mean power of -0.6 dB, is the result obtained

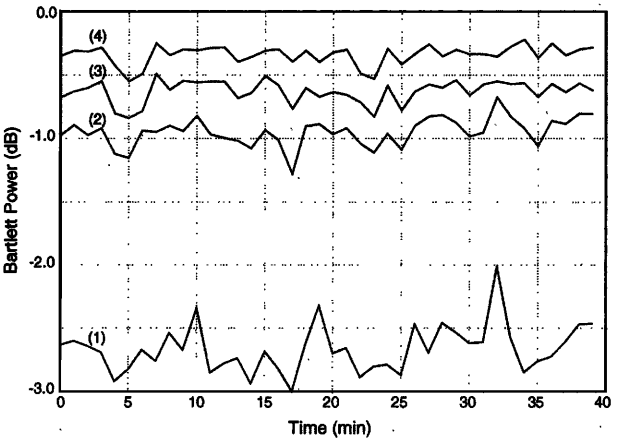

FIG. 7. Bartlett power at the surface maximum as a function of time for the stationary source using: (1) baseline model; (2) baseline with GA estimated bathymetry=128.9 m and receiver depth=111.7 m; (3) baseline with GA estimated bathymetry=128.9 m, receiver depth=111.7 m and sediment parameters; and (4) all GA estimated parameters (search region 5 to 6 km, 10–100 m).

using the baseline model augmented with the GA estimated values for bathymetry, receiver depth, and the sediment parameters. Finally, line (4) provides the Bartlett power when all of the GA model parameters were used. For this case the mean Bartlett power was -0.3 dB. Since 0 dB represents a perfect match, this implies that the GA estimated parameters provided a good fit to the actual environmental parameters at the trial site at this frequency.

B. Source localization

Ambiguity surfaces were computed over a search region of 1 to 10 km in range ($\Delta r=62.4$ m) and 10 to 100 m in depth ($\Delta d=0.625$ m) using the baseline model and the GA estimated model for all 40 time samples. Figure 8 illustrates an ambiguity surface calculated using an 8-s data sample for

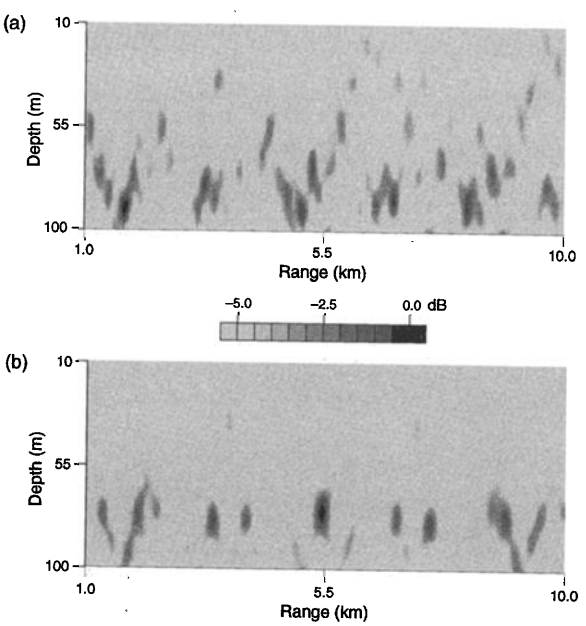

FIG. 8. Range/depth ambiguity surface for the stationary source using (a) baseline model and (b) GA estimated model, at $T=0$ min.

both the baseline model and the GA estimated model. All ambiguity surfaces looked essentially identical to these two surfaces. The maximum of the ambiguity surfaces, using the GA estimated model, was constant at 5430 m in range and 75.6 m in depth for all 40 time samples. This source location estimate was quite close to the actual. As previously discussed the actual source location was predicted to be 5600 ± 200 m in range and 80 ± 2 m in depth. The maximum-to-largest sidelobe ratio was about 1 dB for all 40 time samples. For the surfaces based on the baseline model the maximum was at 1748 m in range and 90.6 m in depth for almost all of the surfaces. The second largest maximum was located at 6803 and 86 m, there was not a local maximum near the source location. Comparing the two ambiguity surfaces it is apparent that the sidelobe structure was reduced substantially when the GA estimated parameters were used.

The use of the estimated forward model parameters improved the localization for the stationary source. Even in a region such as the North Elba site where a good average geoacoustic model had previously been estimated, the source localization was improved considerably through the use of inversion of the acoustic data for forward model parameters. Figure 7 clearly illustrated that accurate estimates of the receiver depth and bathymetry were very important.

IV. MOVING SOURCE LOCALIZATION

On the afternoon of 27 October 1993 a source was towed from point A to point B (Fig. 1) at a speed of approximately 3.5 kn. The depth of the source was monitored on board the source ship using a pressure sensor mounted on the source. The range of the source ship from the vertical array was estimated using GPS positions recorded on board. A PRN signal with a center frequency of 170 Hz was transmitted for about 20 min. Every minute a transmission lasting 30 s was sent out. Eighteen samples of this signal have been analyzed in the same manner as the stationary source data. Cross-spectral matrices based on an 8-s observation were computed at 1-min intervals.

Ambiguity surfaces were computed for the 18 time samples using the baseline and GA estimated model parameters. The surfaces were computed over a search region of 5 to 10 km in range ($\Delta r = 62.4$ m) and 10 to 100 m in depth ($\Delta d = 0.625$ m). For each time sample the range and depth positions for the surface maximum were used as the source location estimates. Figure 9 illustrates these estimates as a function of time along with the actual positions for the source ship. Only those estimates that were within the expected source range interval (5 to 8 km) and depth interval (60 to 80 m) are plotted. The Bartlett power corresponding to those estimates within that range/depth region is also provided.

It is seen from Fig. 9(a) that the range estimates based on the baseline model were fairly sparse. Only 8 of the 18 estimates were within the range/depth region, and for those there was a bias of 500 to 800 m. The range estimates based on the GA estimated model were consistent; only one estimate fell outside of the range/depth region. The bias in the range estimates was reduced to about 300 to 400 m. Figure

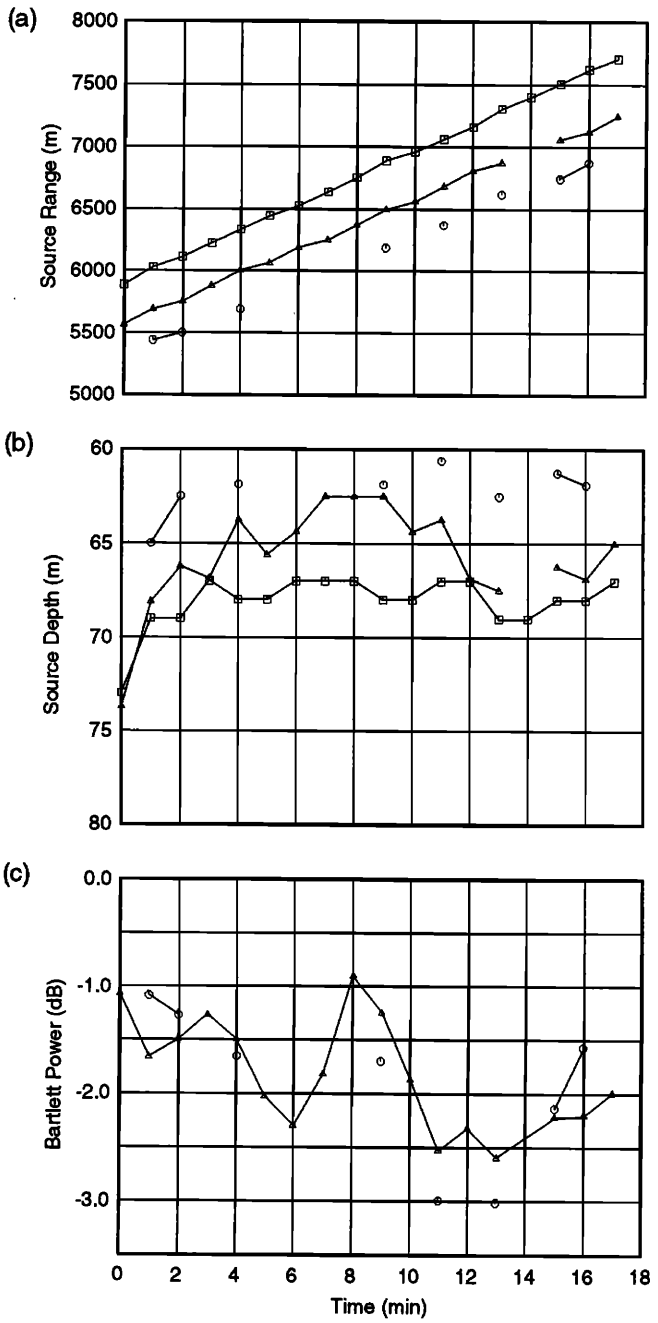

FIG. 9. Source locations and Bartlett power as a function of time. Actual source locations (squares), estimated source locations based on GA estimated model (triangles) and estimated source locations based on baseline model (circles) for the moving source: (a) range (b) depth, and (c) Bartlett power.

9(b) illustrates the depth estimates. Again the depth estimates based on the baseline model are sparse and do not track the actual source depth. The estimates based on the GA estimated model are quite good. In particular, note the estimates within the first 4 min where the source is coming up; the matched-field estimates track the actual positions well.

Figure 10 illustrates examples of ambiguity surfaces computed using the moving source data for two time samples, one at the beginning of the data set and one near the end. The one at $T = 0$ min corresponds to a case where the maximum of the surface for the baseline model is not at or

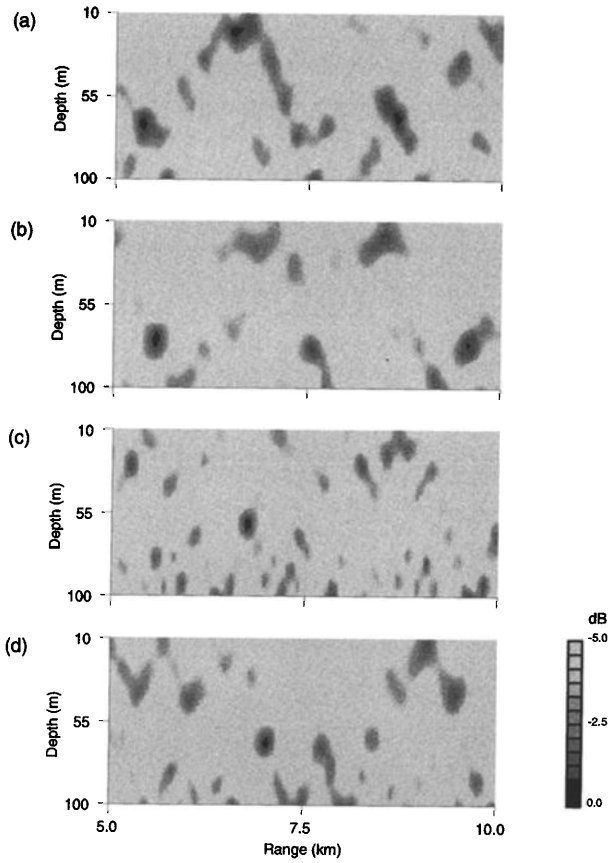

FIG. 10. Range/depth ambiguity surfaces for the moving source calculated using the baseline and GA estimated models of Table II; (a) baseline model at $T=0$ min, (b) GA estimated model at $T=0$ min, (c) baseline model at $T=15$ min, and (d) GA estimated model at $T=15$ min.

near to the source location. For the one at $T=15$ min the maximum for the baseline model is near to the source location. In both cases the sidelobe level was reduced when the GA estimated model parameters were used.

V. CONCLUSIONS

Acoustic field data and environmental data were collected in shallow water in October 1993. A vertical receive array with acoustic array positioning was used along with a stationary and moving source. These data were used to evaluate the performance of field inversion methods for the estimation of environmental and source location parameters.

Genetic algorithms were first applied for the estimation of the geometric and geoacoustic parameters. Highly consistent estimates for bathymetry, receiver depths, and compressional speed in the bottom were obtained. Reasonable estimates were obtained for the other environmental parameters. These estimates were used for the forward model parameters required for performing matched-field source localization. Specifically, field observations for a stationary source were used to invert for the forward model parameters that are required to support matched-field source localization. The estimated forward model parameters were then used in a standard Bartlett processor to accurately localize a moving source in range and depth over a range interval of 5.8 to 7.7 km. The use of the GA estimated geometric and geoacoustic parameters improved the source localization performance considerably.

The application of global methods, specifically genetic algorithms, for estimation of the forward model parameters to support source localization has been shown to be effective for a range-independent shallow water environment.

A reviewer raised the question relative to the applicability of GA for range-dependent environments, in particular relative to the computational feasibility of global estimation in a range-dependent environment. A range-dependent version of the GA code has been developed based on adiabatic normal modes. For those environments that can be treated using the adiabatic approximation, the CPU time would increase over the range-independent case, but not greatly; it would increase linearly by the number of range sectors used to describe the environment.

ACKNOWLEDGMENTS

The authors wish to acknowledge the significant contribution of the SACLANT Centre Engineering Department for their diligent preparation and operation of the sea-going equipment and the captain and crew of the R/V ALLIANCE for their outstanding contributions to the sea-going operations. The support of the Italian Navy, in particular the crew of the ITN Palmaria, is also appreciated.

[1] A. B. Baggeroer, W. A. Kuperman, and H. Schmidt, "Matched field processing: Source localization in correlated noise as an optimum parameter estimation problem," J. Acoust. Soc. Am. **83**, 571–587 (1988).
[2] M. J. Hinich and E. J. Sullivan, "Maximum-likelihood passive localization using mode filtering," J. Acoust. Soc. Am. **85**, 214–219 (1989).
[3] J. M. Ozard, "Matched-field processing in shallow water for range, depth, and bearing determination: Results of experiment and simulation," J. Acoust. Soc. Am. **86**, 744–753 (1989).
[4] R. M. Hampson and R. M. Heitmeyer, "Environmental and system effects on source localization in shallow water by the matched-field processing of a vertical array," J. Acoust. Soc. Am. **86**, 1950–1959 (1989).
[5] C. Feuillade, W. A. Kinney, and D. R. DelBalzo, "Shallow-water matched-field localization off Panama City, Florida," J. Acoust. Soc. Am. **88**, 423–433 (1990).
[6] S. M. Jesus, "Broadband matched-field processing of transient signals in shallow water," J. Acoust. Soc. Am. **93**, 1841–1850 (1993).
[7] D. F. Gingras, "Robust broadband matched-field processing: Performance in shallow water," IEEE J. Ocean. Eng. **OE-18**, 224–231 (1993).
[8] A. Tolstoy, O. Diachok, and L. N. Frazer, "Acoustic tomography via matched-field processing," J. Acoust. Soc. Am. **89**, 1119–1127 (1991).
[9] M. D. Collins and W. A. Kuperman, "Focalization: Environmental focusing and source localization," J. Acoust. Soc. Am. **90**, 1410–1422 (1991).
[10] M. D. Collins, W. A. Kuperman, and H. Schmidt, "Nonlinear inversion for ocean-bottom properties," J. Acoust. Soc. Am. **92**, 2770–2783 (1992).
[11] S. E. Dosso, M. L. Yeremy, J. M. Ozard, and N. R. Chapman, "Estimation of ocean-bottom properties by matched-field inversion of acoustic field data," IEEE J. Ocean. Eng. **OE-18**, 232–239 (1993).
[12] C. E. Lindsay and N. R. Chapman, "Matched-field inversion for geoacoustic model parameters using simulated annealing," IEEE J. Ocean. Eng. **OE-18**, 224–231 (1993).
[13] P. Gerstoft, "Inversion of seismoacoustic data using genetic algorithms and *a posteriori* probability distributions," J. Acoust. Soc. Am. **95**, 770–782 (1994).
[14] T. Akal, "Bathymetry and bottom structure of zones near the island of Elba used for acoustical trials in shallow water," TM-162, SACLANT ASW Research Centre, La Spezia, Italy (1970).
[15] T. Akal, C. Gehin, B. Matteucci, and B. Tonarelli "Measured and computed physical properties of sediment cores, Island of Elba zone," M-82, SACLANT ASW Research Centre, La Spezia, Italy (1972).
[16] F. B. Jensen, "Comparison of transmission loss data for different shallow

water areas with theoretical results provided by a three-fluid normal-mode propagation model," in *Sound Propagation in Shallow Water*, edited by O. F. Hastrup and O. V. Olesen (CP-14, SACLANT ASW Research Centre, La Spezia, Italy, 1974), pp. 79–92.

[17] P. Gerstoft and A. Caiti, "Acoustic estimation of bottom parameters: Error bounds by local and global methods," in *Proceedings of the Second European Conference on Underwater Acoustics*, edited by L. Bjørnø (Copenhagen, Denmark, 1994), pp. 887–892.

[18] D. F. Gingras, L. Troiano, and R. B. Williams, "Acoustic array positioning in shallow water," SACLANT Undersea Research Centre, SM-283, La Spezia, Italy (1994).

[19] S. W. Golomb, *Shift Register Sequences* (Holden-Day, San Francisco, CA, 1967).

[20] F. B. Jensen and M. C. Ferla, "SNAP—The SACLANTCEN normal mode propagation model," SACLANT Undersea Research Centre, SM-121, La Spezia, Italy (1979).

[21] D. F. Gingras, "Impact of uncertain environmental knowledge on the shallow-water transfer function," SACLANT Undersea Research Centre, SM-263, La Spezia, Italy (1992).

[22] P. Gerstoft, "Global inversion by genetic algorithms for both source position and environmental parameters," J. Comput. Acoust. **2**, 251–266 (1994).